Deeply virtual Compton Scattering cross section measured with CLAS

Baptiste GUEGAN

PHOTON 2013, Paris, 22/05/13

INSTITUT DE PHYSIQUE NUCLÉAIRE
ORSAY

Deeply Virtual Compton Scattering

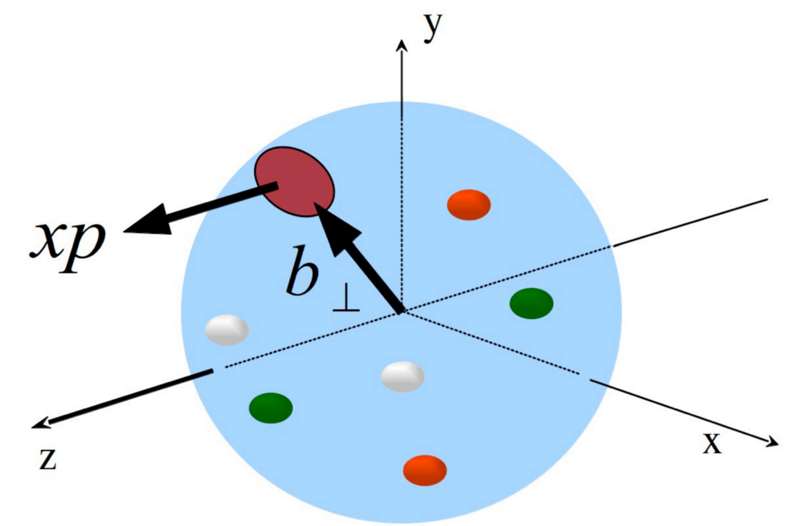

Generalized Parton Distributions (GPD):

→ correlation between x and t

Deeply Virtual Compton Scattering

Generalized Parton Distributions (GPD):

→ correlation between x and t

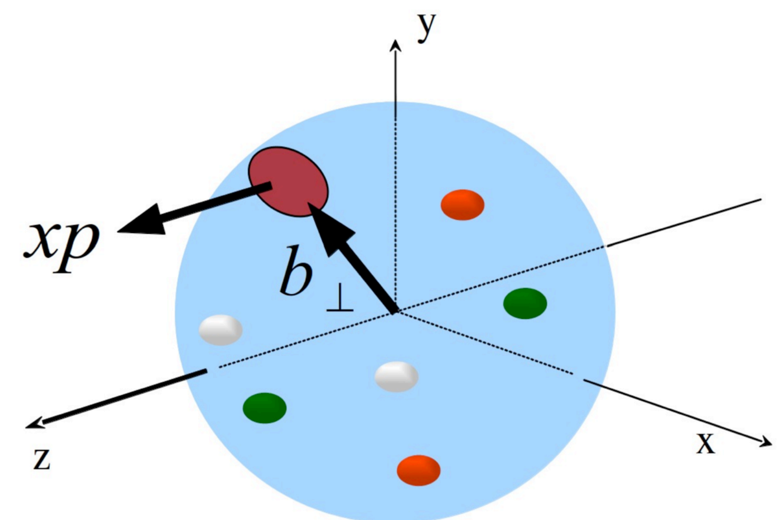

Accessible via Deeply Virtual Compton Scattering:

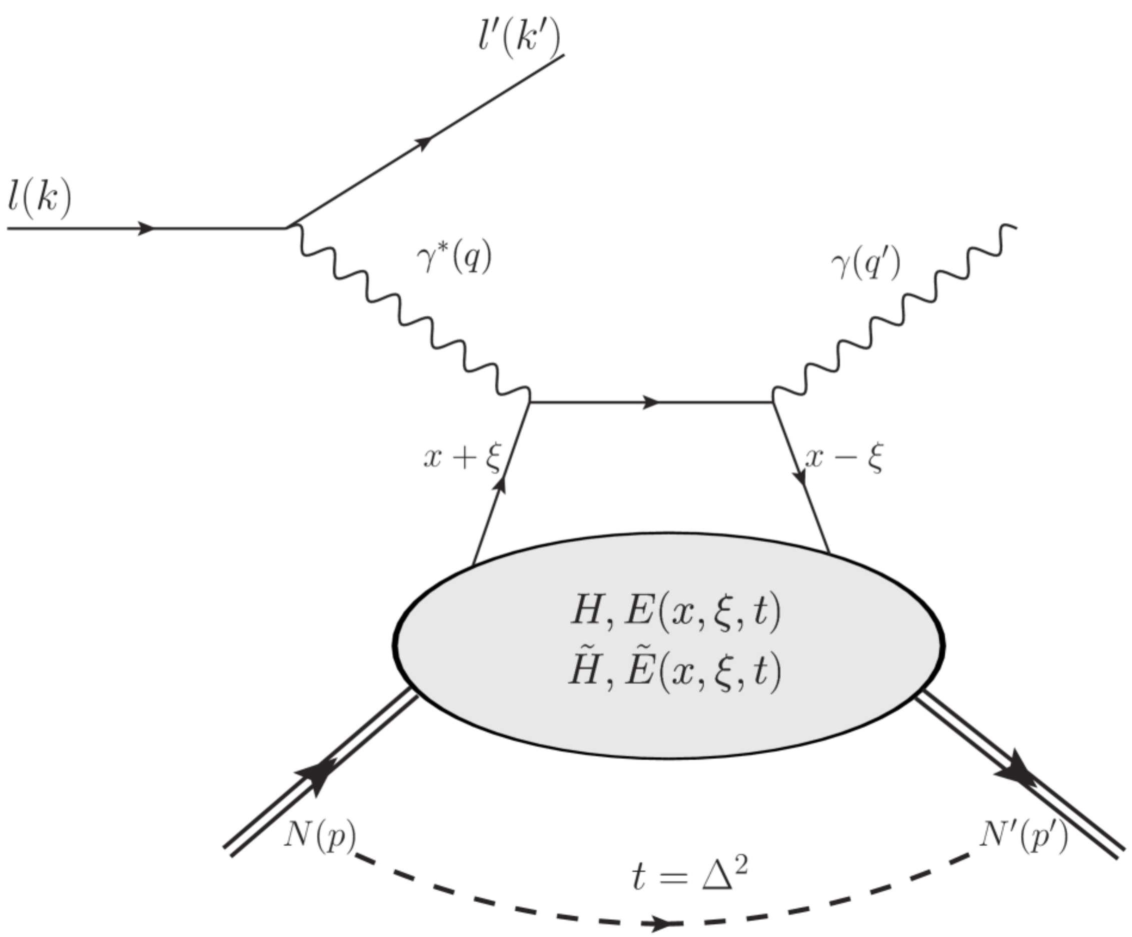

$$\left.\begin{array}{l}(x+\xi)\\(x-\xi)\end{array}\right| \text{ longitudinal momentum fractions of quark}$$

$t = \Delta^2 = (p' - p)^2$: squared momentum transfer

Deeply Virtual Compton Scattering

Generalized Parton Distributions (GPD):

$\rightarrow$ correlation between x and t

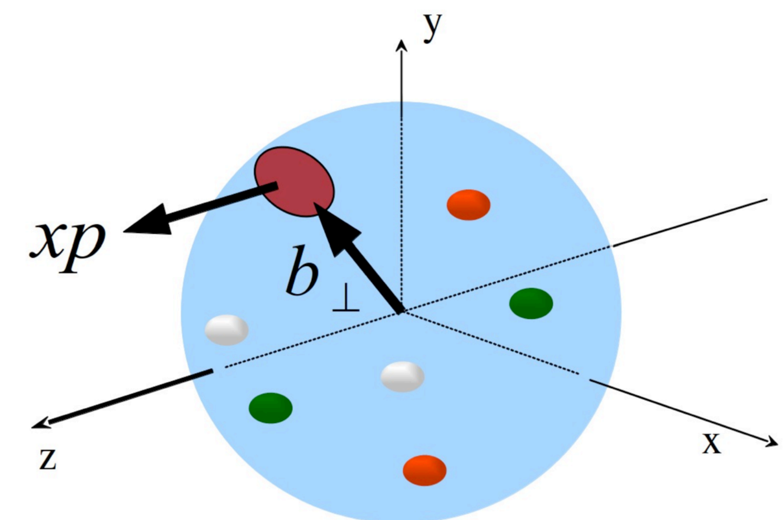

Accessible via Deeply Virtual Compton Scattering:

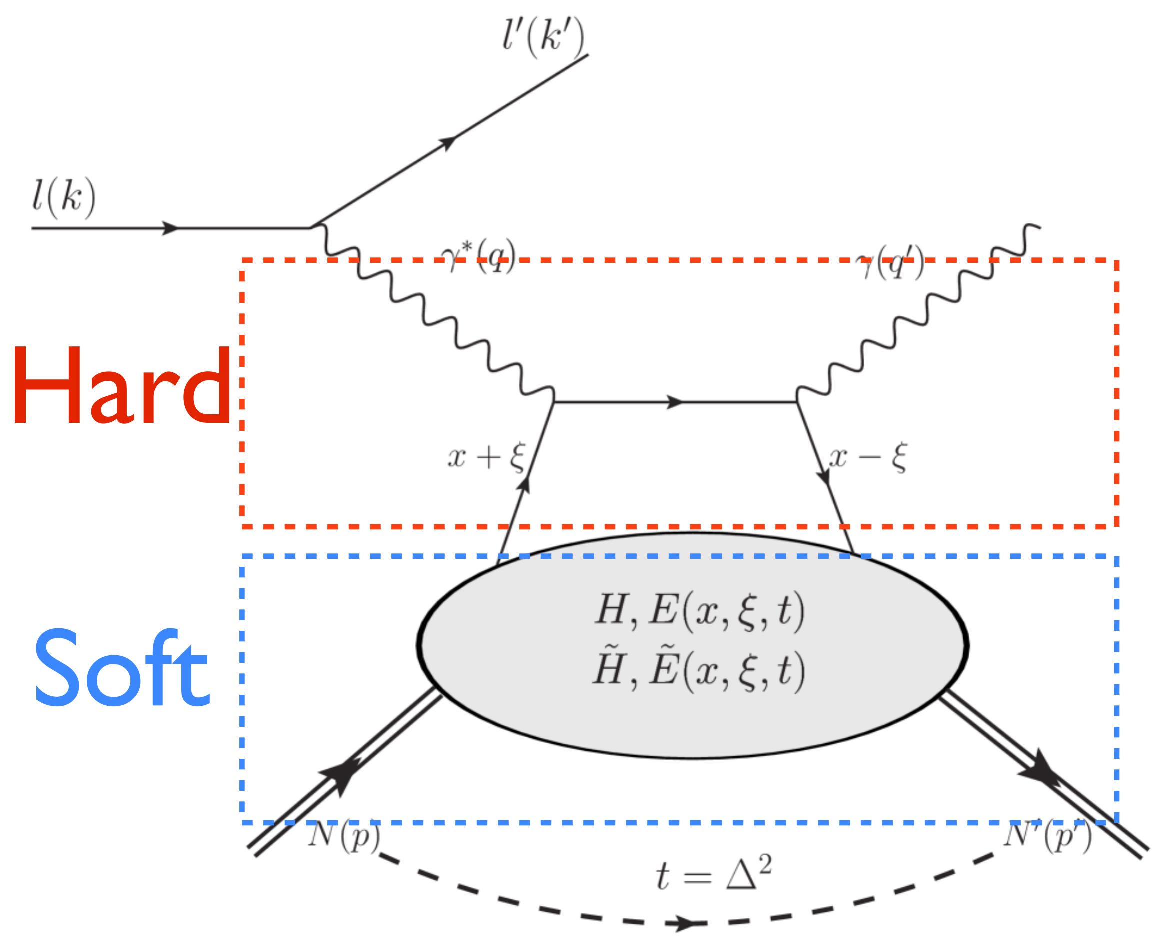

$\left.\begin{array}{l}(x+\xi)\\(x-\xi)\end{array}\right|$ longitudinal momentum fractions of quark

$t = \Delta^2 = (p'-p)^2$: squared momentum transfer

$$x_B = \frac{Q^2}{2p \cdot q} \qquad \xi \approx \frac{x_B}{2 - x_B}$$

At large Q^2, small t and fixed x_B , the process can be factorized and described by 4 Generalized Parton Distributions

Exclusive electroproduction of a photon

Contribution from both DVCS and Bethe-Heitler (undistinguishable experimentally):

$$\sigma_{(ep \to ep\gamma)} \propto |T^{DVCS} + T^{BH}|^2$$

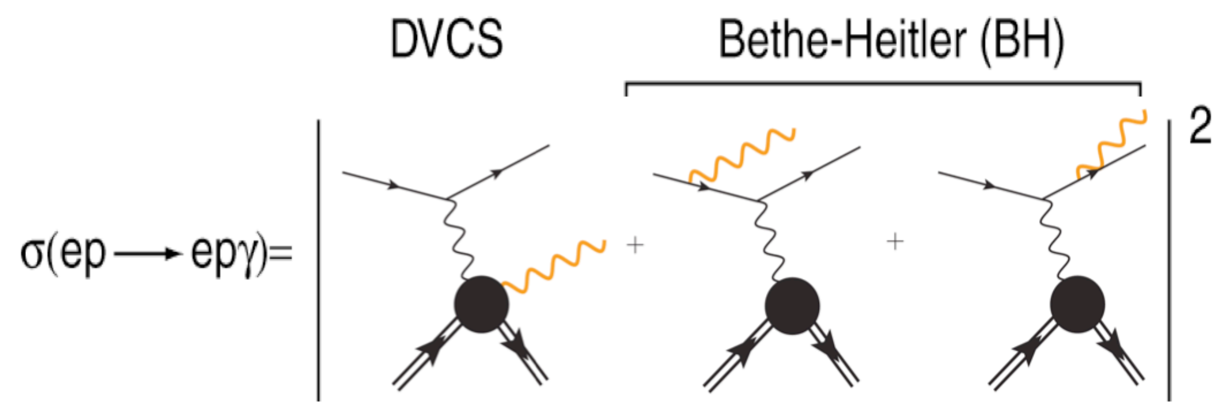

- T^{BH} : At low t, the nucleon FFs (Dirac, Pauli) are well known so that T^{BH} is precisely calculable
- $T^{DVCS} \propto \int_{-1}^{1} dx \frac{GPD(x,\xi,t)}{x \pm \xi \mp i\epsilon} = \mathcal{P}\int_{-1}^{1} dx \frac{\boxed{GPD(x,\xi,t)}}{x \pm \xi} \pm i\pi \boxed{GPD(x = \mp\xi, \xi, t)}$

  $\rightarrow$ GPDs appear in the real part through an integral over x

  $\rightarrow$ GPDs appear in the imaginary part at the lines $x = \pm\xi$

Exclusive electroproduction of a photon

Contribution from both DVCS and Bethe-Heitler (undistinguishable experimentally):

$$\sigma_{(ep \to ep\gamma)} \propto \left| T^{DVCS} + T^{BH} \right|^2$$

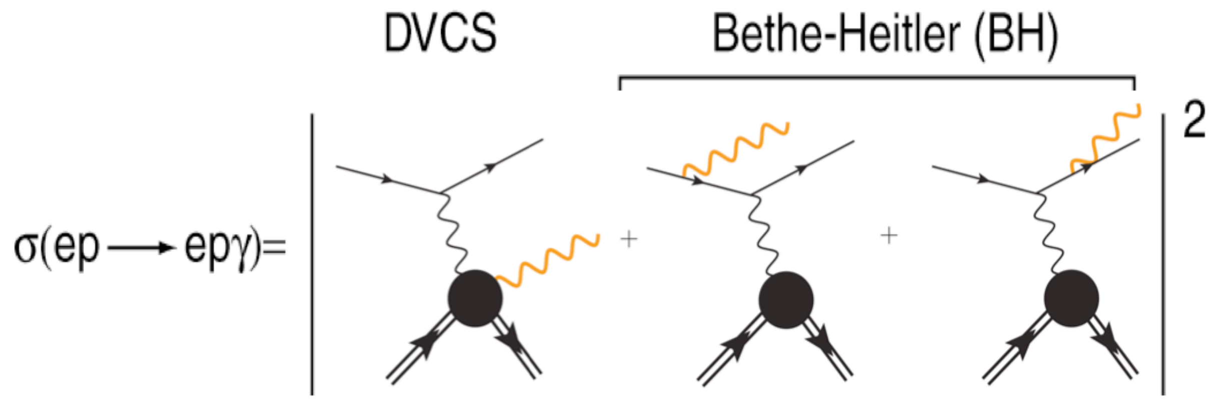

- T^{BH} : At low t, the nucleon FFs (Dirac, Pauli) are well known so that T^{BH} is precisely calculable
- $T^{DVCS} \propto \int_{-1}^{1} dx \frac{GPD(x,\xi,t)}{x \pm \xi \mp i\epsilon} = \mathcal{P} \int_{-1}^{1} dx \frac{\boxed{GPD(x,\xi,t)}}{x \pm \xi} \pm i\pi \boxed{GPD(x = \mp\xi, \xi, t)}$

  → GPDs appear in the real part through an integral over x

  → GPDs appear in the imaginary part at the lines $x = \pm\xi$

With a polarized beam and an unpolarized target, one can measure 2 observables:

- $\frac{d^4\sigma}{dt dQ^2 dx_B d\phi} \propto \left|T^{BH}\right|^2 + 2T^{BH} \boxed{\mathrm{Re}(T^{DVCS})} + \left|T^{DVCS}\right|^2$
- $\frac{d^4\overrightarrow{\sigma} - d^4\overleftarrow{\sigma}}{dt dQ^2 dx_B d\phi} \propto 2T^{BH} \boxed{\mathrm{Im}(T^{DVCS})} + \left[\left|T^{\overrightarrow{DVCS}}\right|^2 - \left|T^{\overleftarrow{DVCS}}\right|^2\right]$

DVCS experiment

- One experiment with two data set: e1-dvcs1 (2005) H-S.Jo, and e1-dvcs2 (2008)
- CLAS + dedicated equipment (IC electromagnetic calorimeter + solenoid)

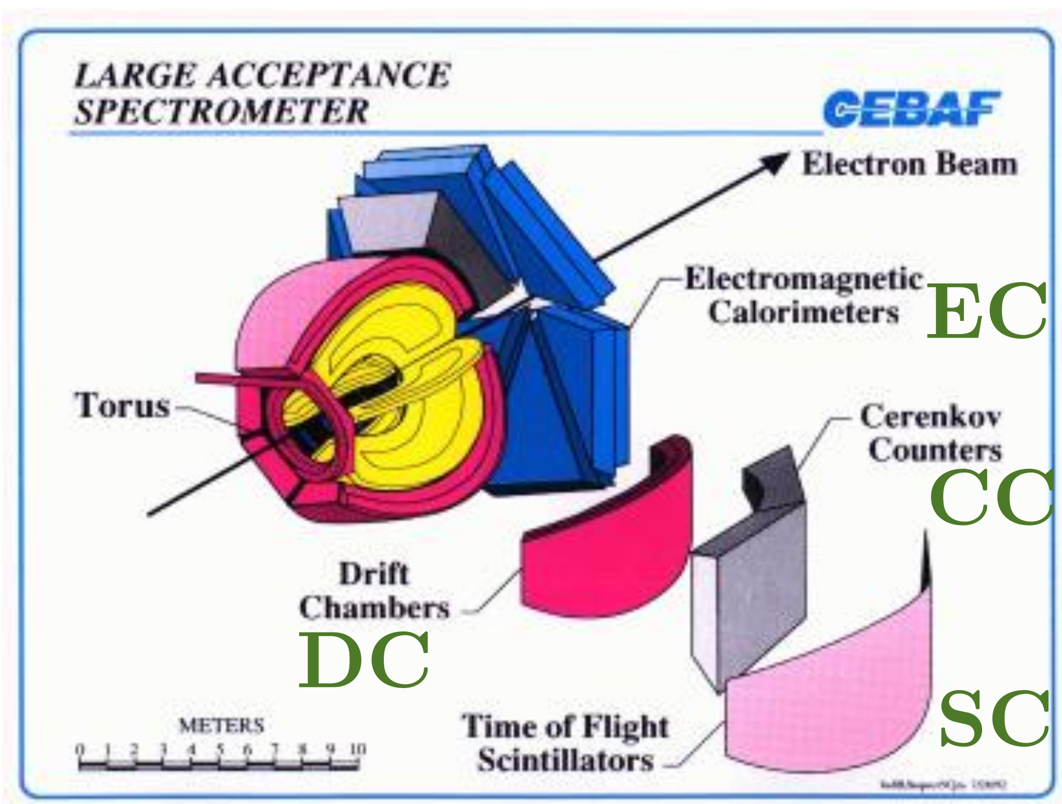

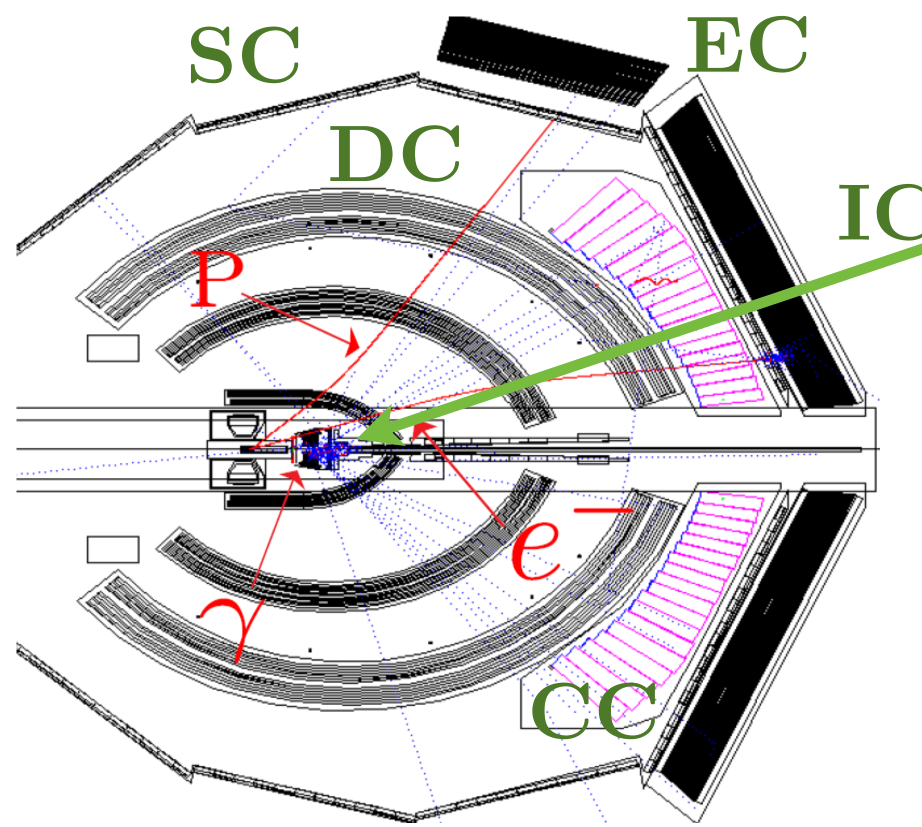

lead tungstate crystals + APD readout

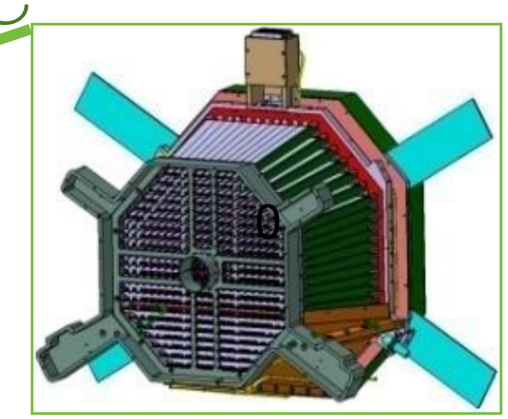

DVCS photons are mostly emitted at forward angles

Beam energy: 5.88 GeV
Beam polarization: 82-87%
Beam current: 20nA

DVCS analysis steps

- Identification of the final-state particles: e, p, γ

$$\Delta\beta = \beta^{SC}_{measured} - \beta^{DC}_{calculated}(M_p) = \frac{d}{ct} - \frac{p}{\sqrt{p^2 + M_p^2}}$$

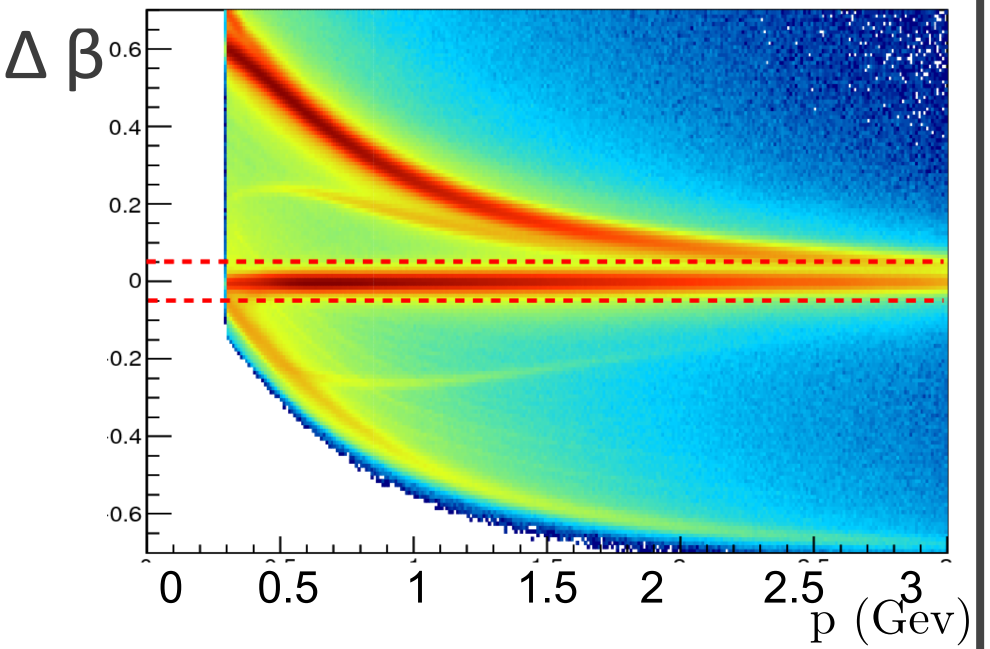

DVCS analysis steps

- Identification of the final-state particles: e, p, γ
- Exclusivity selection of the DVCS channel

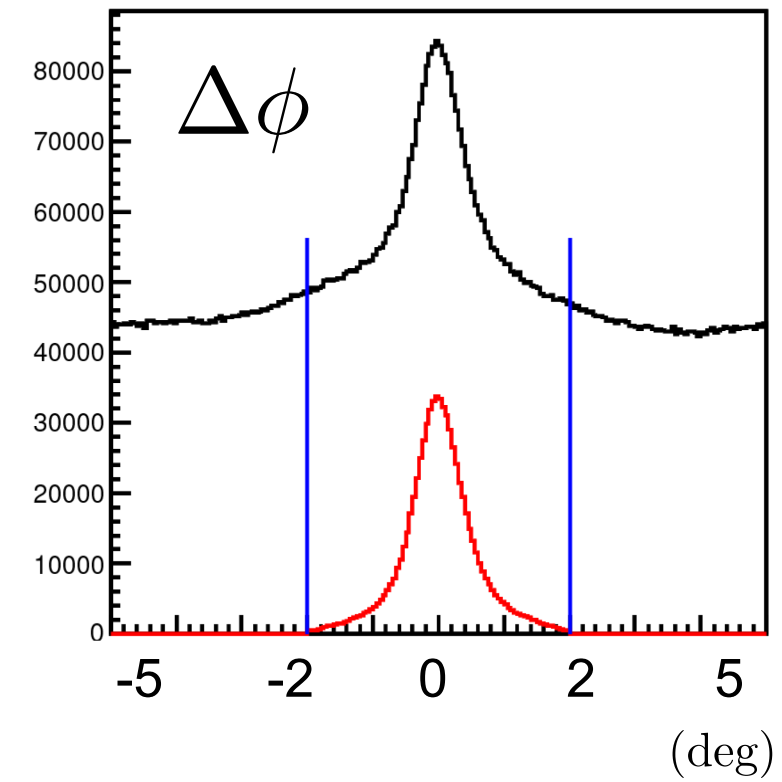

DVCS analysis steps

- Identification of the final-state particles: e, p, γ
- Exclusivity selection of the DVCS channel
- Evaluation of the contamination of the DVCS channel by the π^0 when one of the two photons is undetected: $ep \to ep\pi^0 \to ep\gamma(\gamma)$

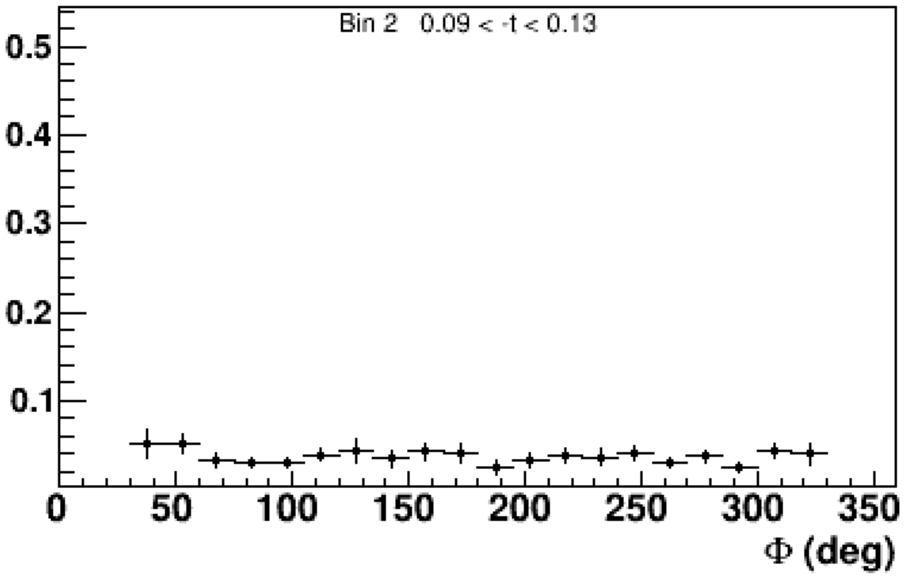

DVCS analysis steps

- Identification of the final-state particles: e, p, γ
- Exclusivity selection of the DVCS channel
- Evaluation of the contamination of the DVCS channel by the π^0 when one of the two photons is undetected: $ep \to ep\pi^0 \to ep\gamma(\gamma)$
- Acceptance computation: $\frac{N^{REC}_{ep\gamma}\ MC}{N^{GEN}_{ep\gamma}\ MC}$

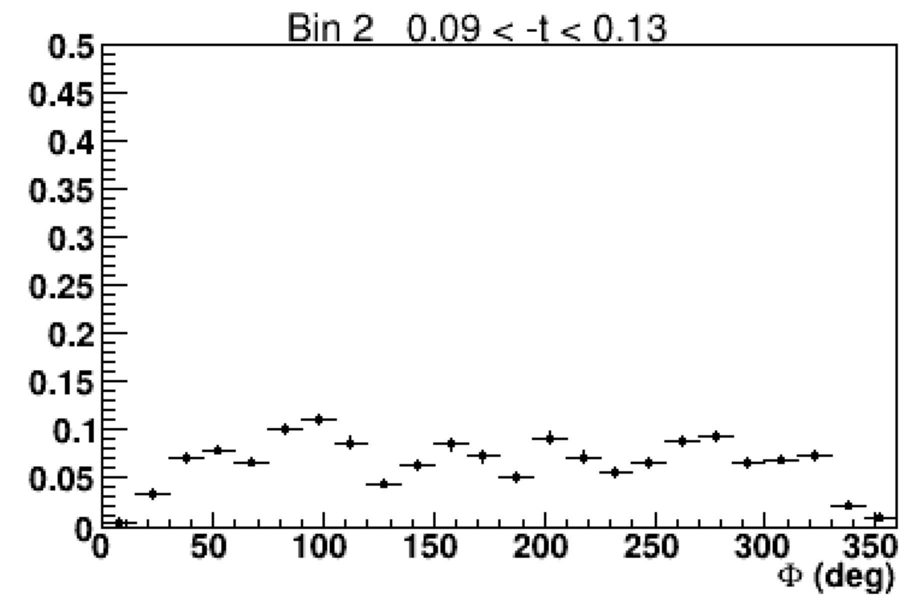

DVCS analysis steps

- Identification of the final-state particles: e, p, γ
- Exclusivity selection of the DVCS channel
- Evaluation of the contamination of the DVCS channel by the π^0 when one of the two photons is undetected: $ep \to ep\pi^0 \to ep\gamma(\gamma)$
- Acceptance computation: $\frac{N^{REC}_{ep\gamma}\ MC}{N^{GEN}_{ep\gamma}\ MC}$
- The integrated luminosity for the whole DVCS2 data set

DVCS analysis steps

- Identification of the final-state particles: e, p, γ
- Exclusivity selection of the DVCS channel
- Evaluation of the contamination of the DVCS channel by the π^0 when one of the two photons is undetected: $ep \to ep\pi^0 \to ep\gamma(\gamma)$
- Acceptance computation: $\frac{N_{ep\gamma}^{REC}\ MC}{N_{ep\gamma}^{GEN}\ MC}$
- The integrated luminosity for the whole DVCS2 data set
- Hyper-volume computation of the bins

DVCS analysis steps

- Identification of the final-state particles: e, p, γ
- Exclusivity selection of the DVCS channel
- Evaluation of the contamination of the DVCS channel by the π^0 when one of the two photons is undetected: $ep \to ep\pi^0 \to ep\gamma(\gamma)$
- Acceptance computation: $\dfrac{N^{REC}_{ep\gamma}\ MC}{N^{GEN}_{ep\gamma}\ MC}$
- The integrated luminosity for the whole DVCS2 data set
- Hyper-volume computation of the bins
- The radiative corrections calculated in each bin in order to compute the cross section at the Born term: ~ 20 % in the BH approximation

Kinematic coverage of the e1-DVCS data and binning

$Q^2 > 1\,GeV^2,\ W > 2\,GeV,\ 21° < \theta_e < 45°,\ p_e > 0.8\,GeV$

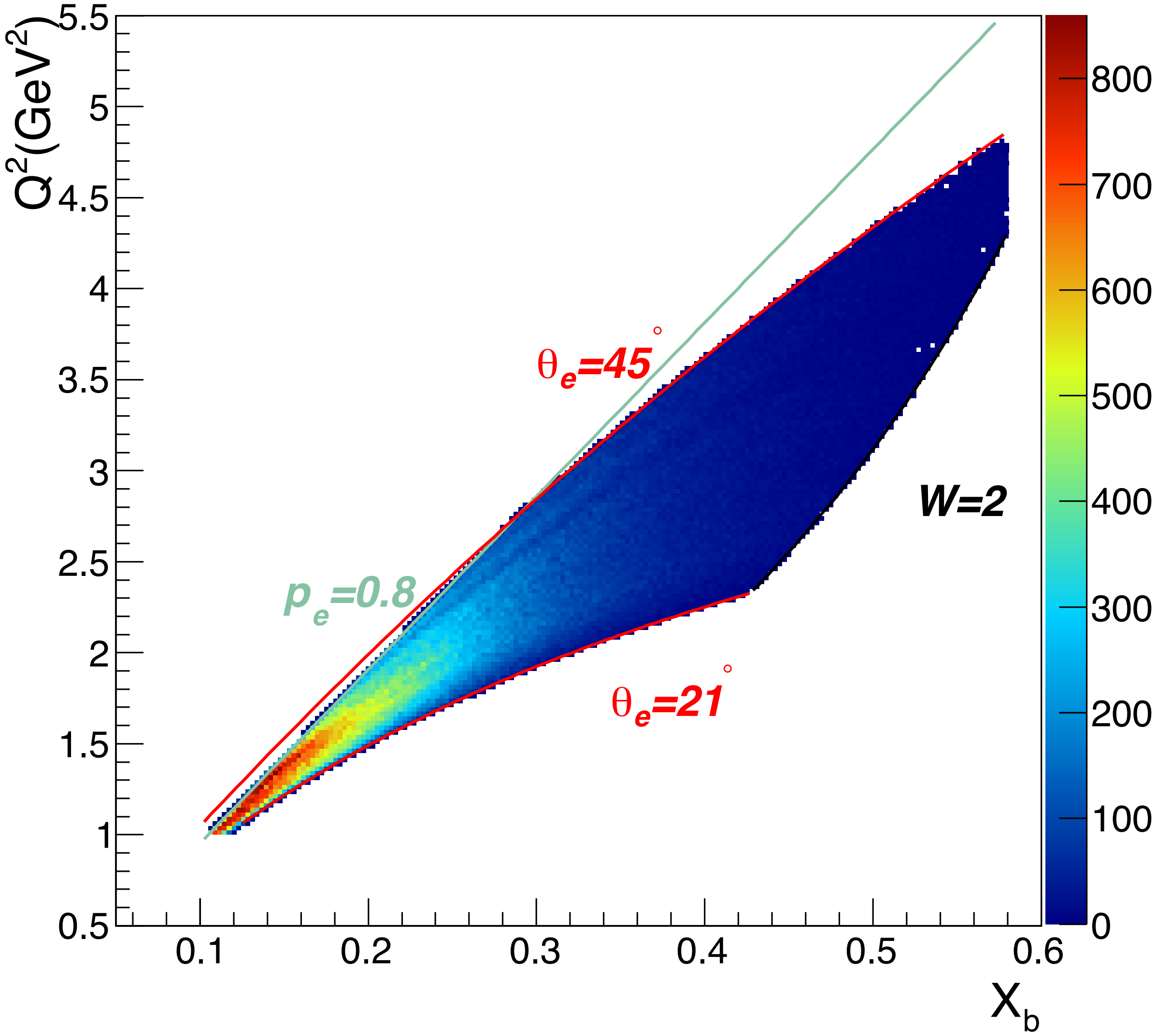

The kinematics of the DVCS reaction is defined by 4 independent variables :

$$Q^2, x_B, -t, \Phi$$

$\rightarrow$ 4-dimensional binning

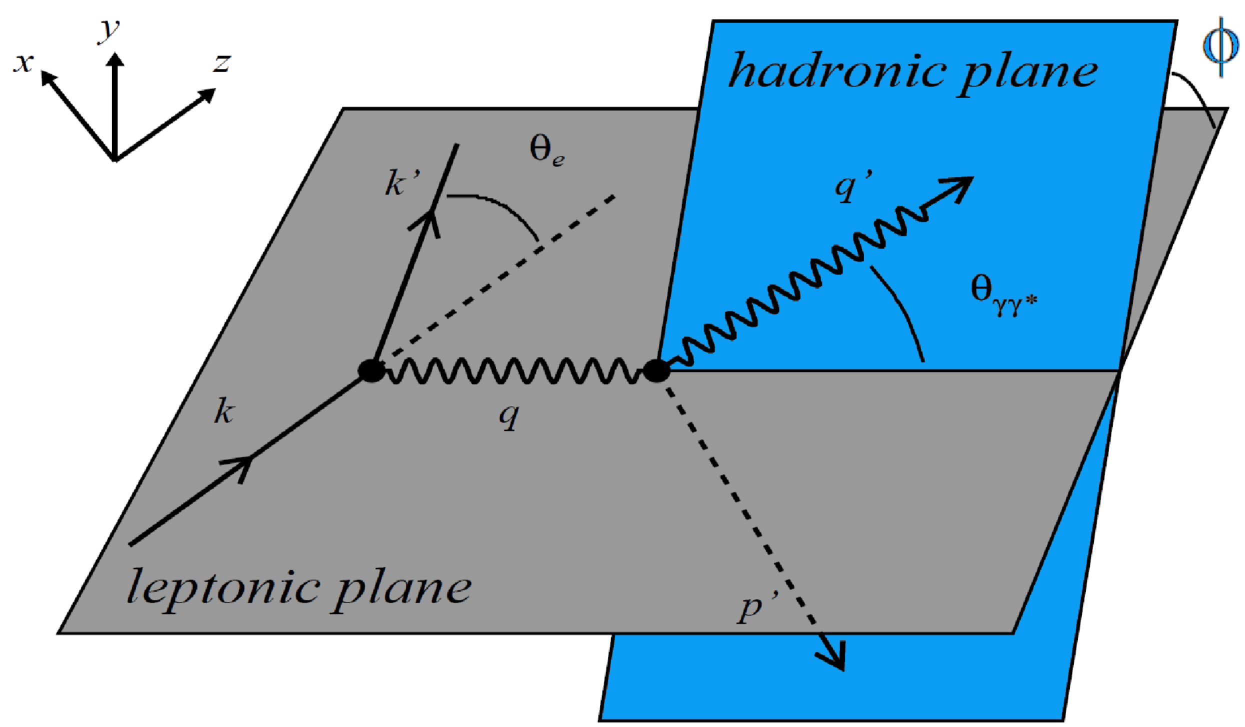

Kinematic coverage of the e1-DVCS data and binning

$Q^2 > 1\,GeV^2,\ W > 2\,GeV,\ 21° < \theta_e < 45°,\ p_e > 0.8\,GeV$

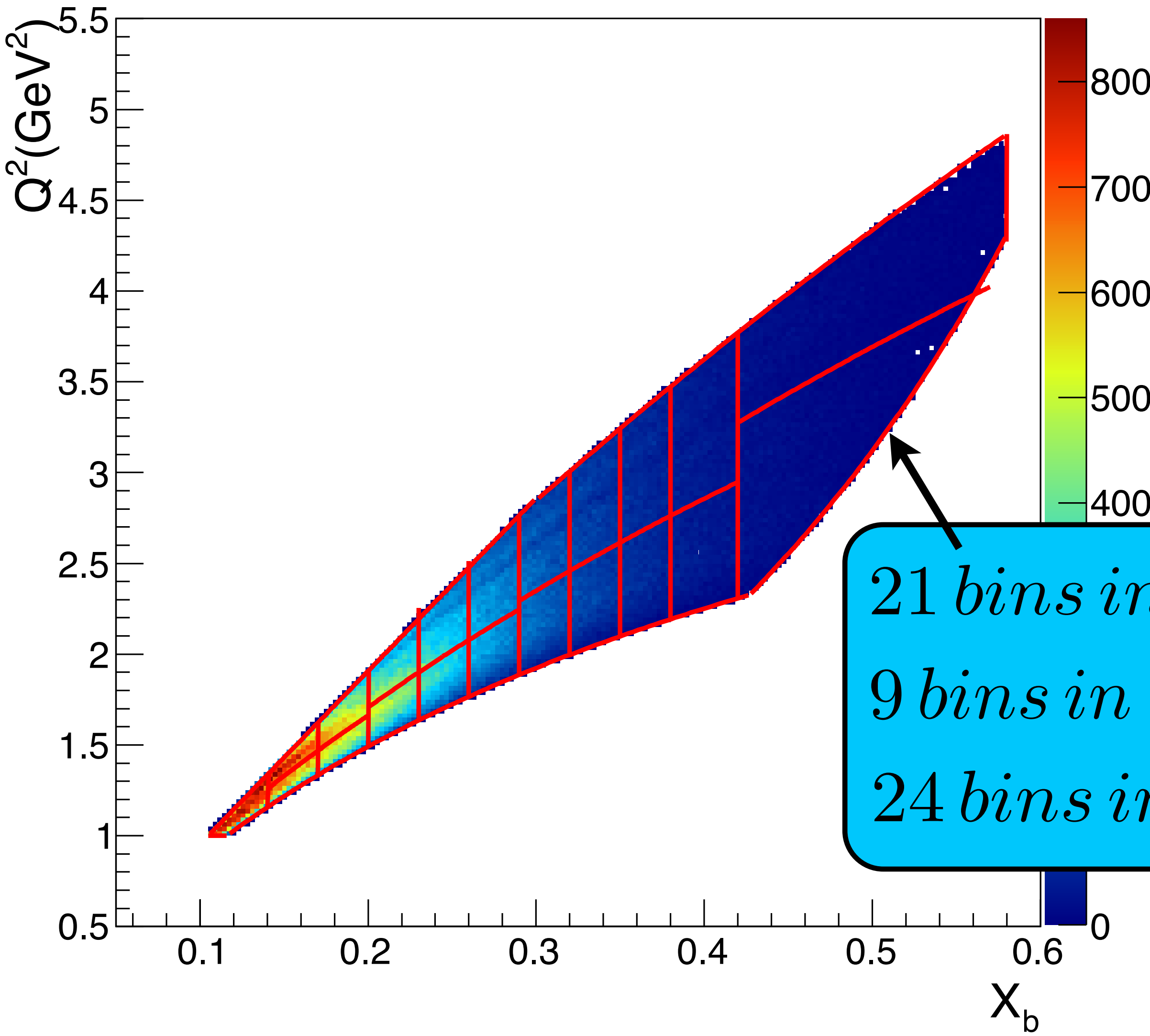

$21\,bins\,in\,(Q^2, x_B)$

$9\,bins\,in\ -t$

$24\,bins\,in\,\Phi$

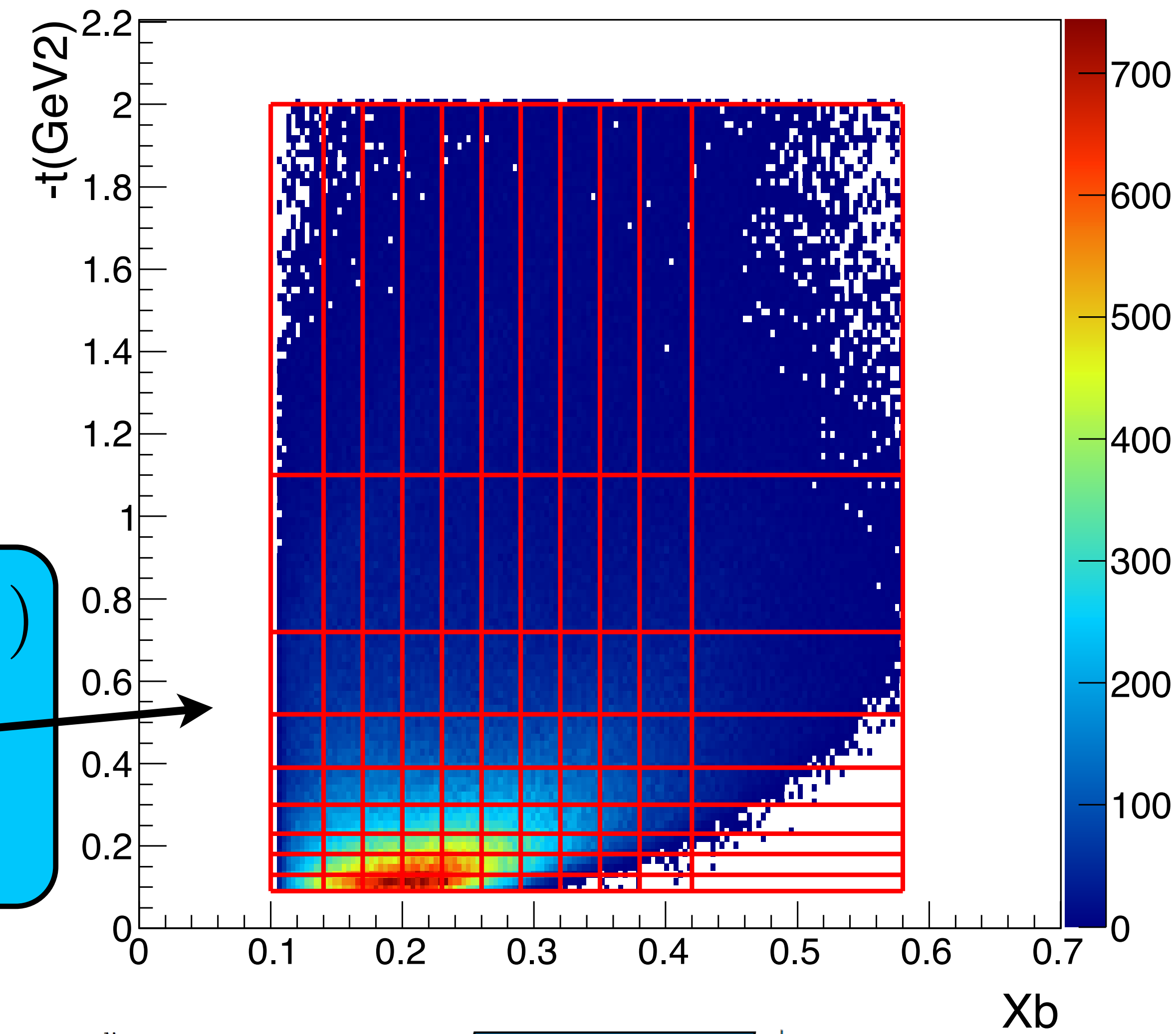

The kinematics of the DVCS reaction is defined by 4 independent variables :

$$Q^2, x_B, -t, \Phi$$

$\rightarrow$ 4-dimensional binning

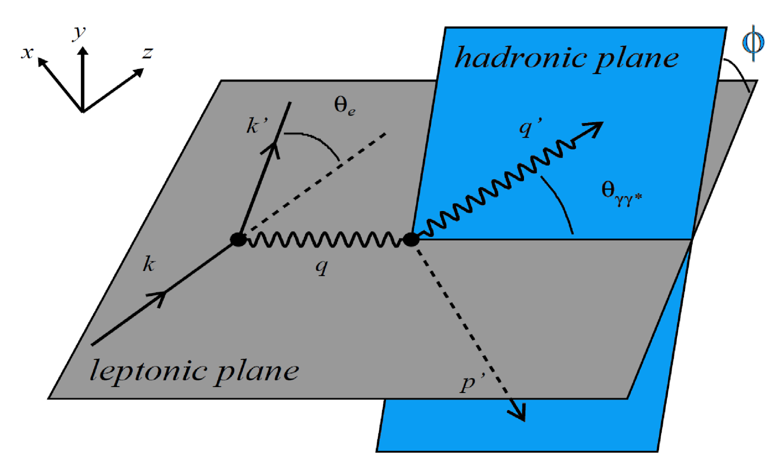

DVCS differential cross section

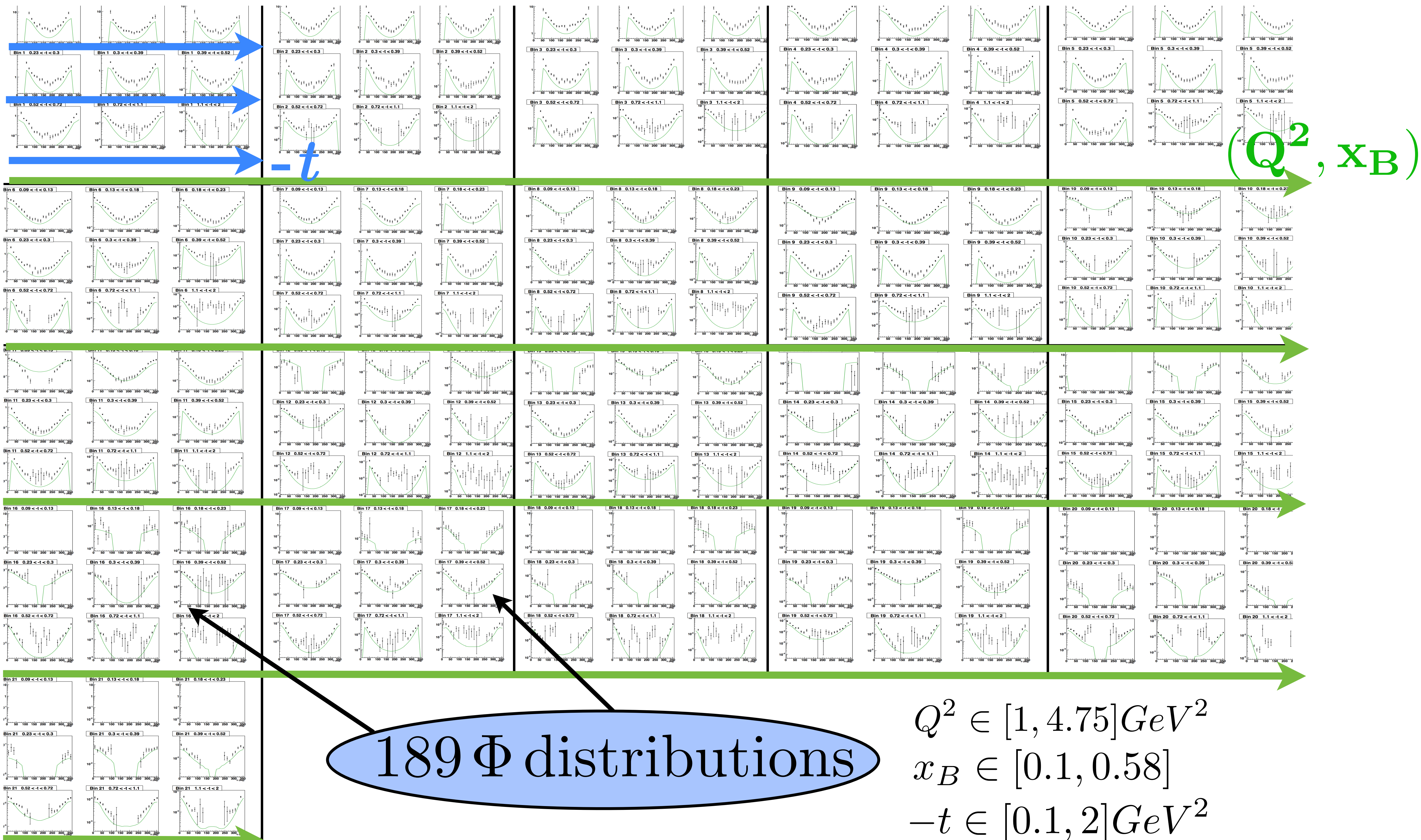

$Q^2 \in [1, 4.75] GeV^2$
$x_B \in [0.1, 0.58]$
$-t \in [0.1, 2] GeV^2$

DVCS differential cross section

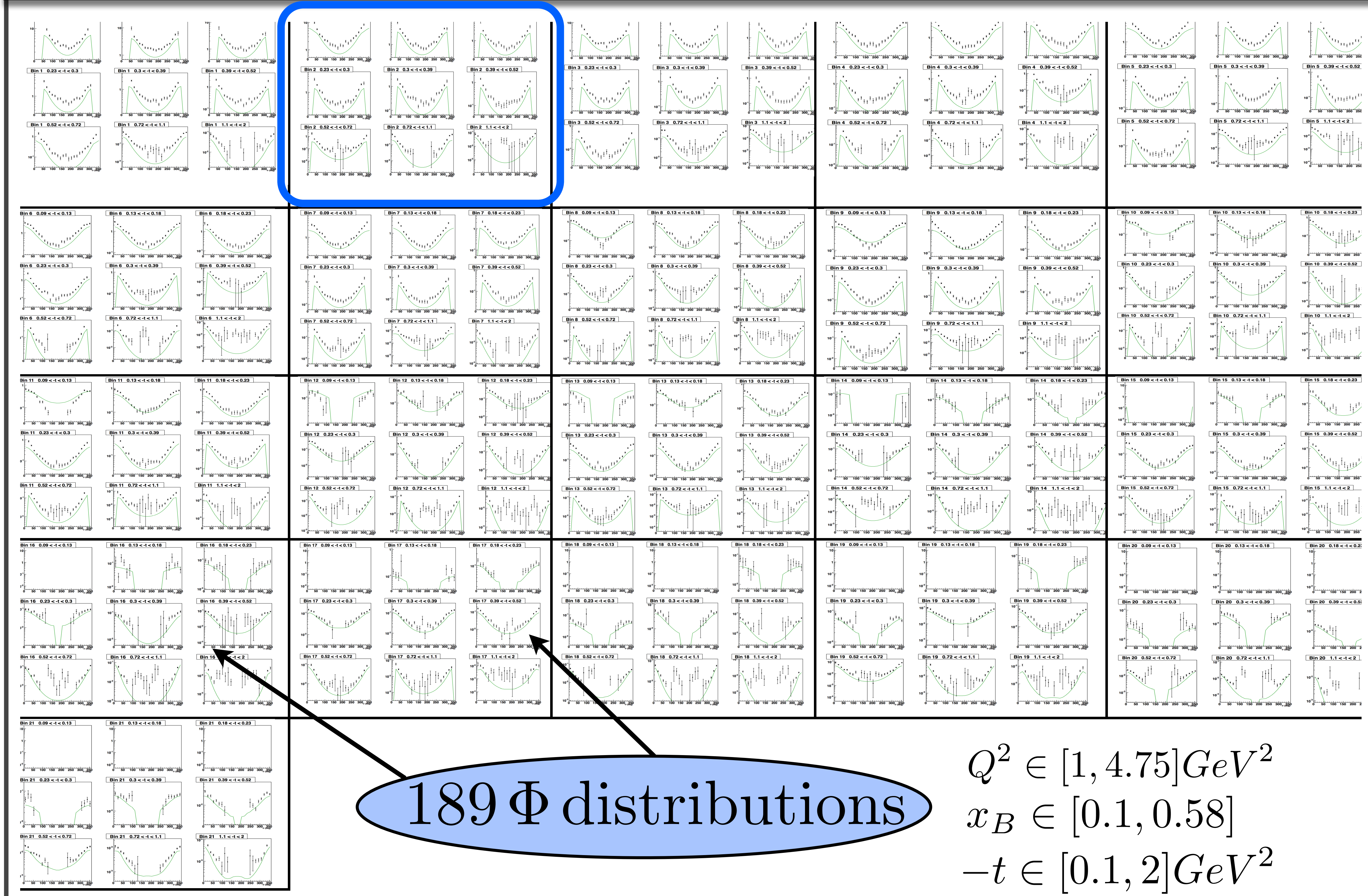

$Q^2 \in [1, 4.75] GeV^2$

$x_B \in [0.1, 0.58]$

$-t \in [0.1, 2] GeV^2$

Unpolarized cross section

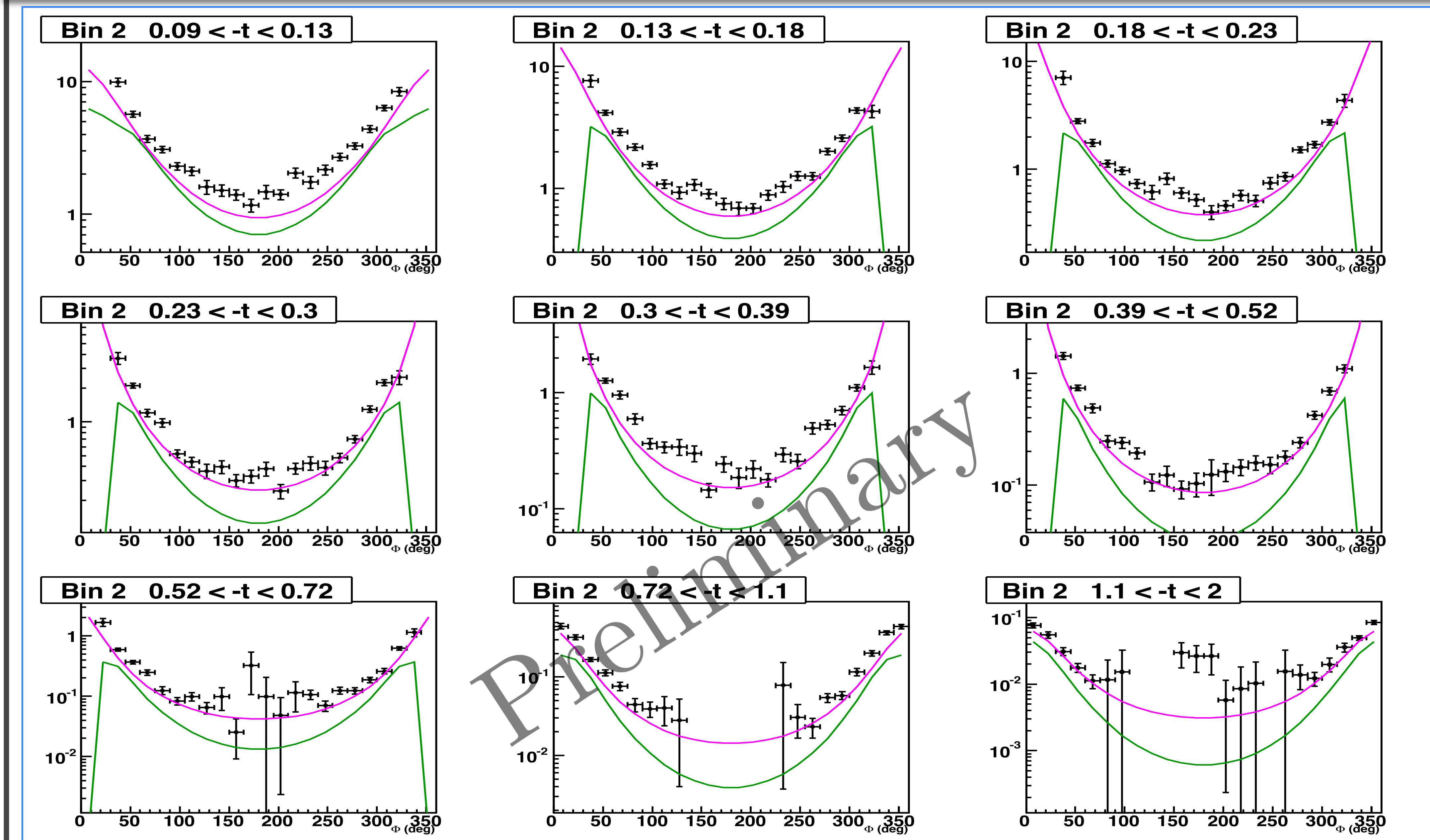

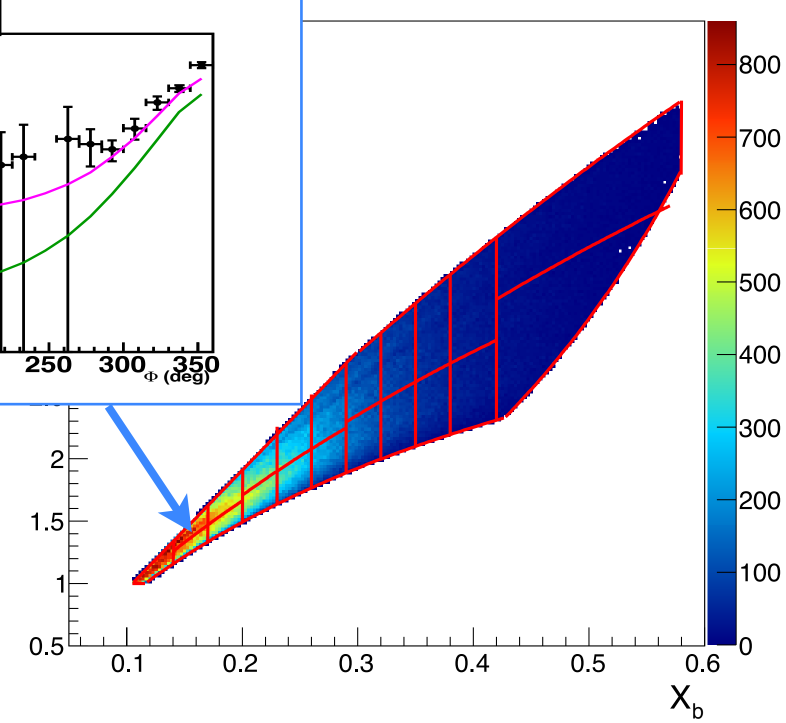

● $\dfrac{d^4\sigma_{ep\to ep\gamma}}{dQ^2\, dx_B\, dt\, d\Phi}$ (nb/GeV^4)

VGG

Bethe-Heitler

M. Vanderhaeghen
P.A.M. Guichon,
M. Guidal

Difference of polarized cross sections

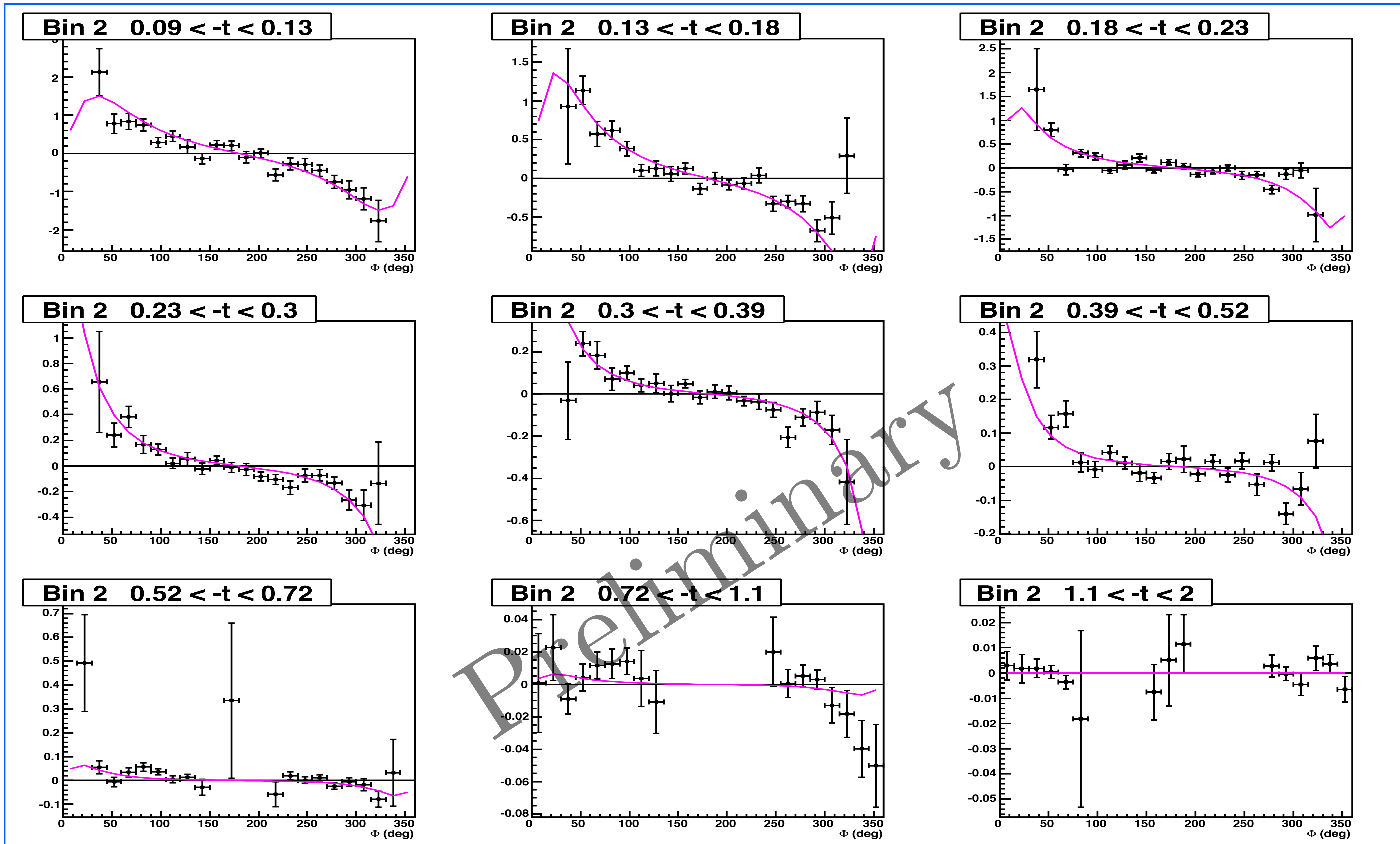

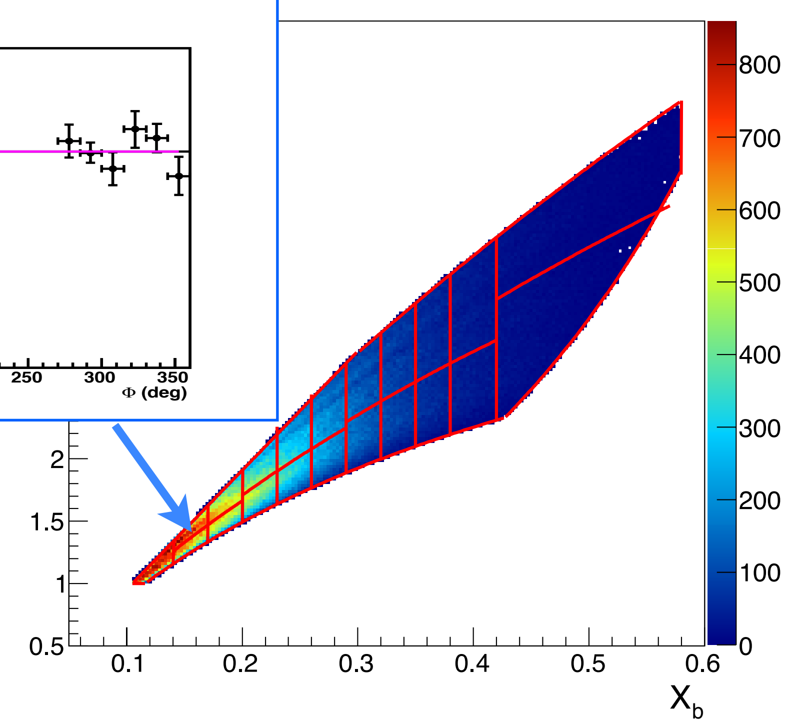

- $$\frac{1}{2}\left(\frac{d^4\sigma^{\rightarrow}_{ep\to ep\gamma}}{dQ^2\,dx_B\,dt\,d\Phi} - \frac{d^4\sigma^{\leftarrow}_{ep\to ep\gamma}}{dQ^2\,dx_B\,dt\,d\Phi}\right)\ (nb/GeV^4)$$ —— VGG

$$= \sin(\Phi)\,\Gamma_\Phi\,\Im m\left[F_1\mathcal{H} + \xi(F_1+F_2)\tilde{\mathcal{H}} - \frac{t}{4M^2}F_2\mathcal{E}\right]$$

Extraction of Compton Form Factors (CFFs)

Quasi-model-independent fitting procedure (M. Guidal, Eur. Phys. J. A 37, 319 (2008)):

→ One does not extract the GPDs, but associated quantities called Compton Form Factors

$$\mathcal{T}^{DVCS} \propto \int_{-1}^{1} dx \frac{GPD(x,\xi,t)}{x \pm \xi \mp i\epsilon} = \mathcal{P}\int_{-1}^{1} dx \frac{GPD(x,\xi,t)}{x \pm \xi} \pm i\pi GPD(x = \mp\xi, \xi, t)$$

Real part **Imaginary part**

→ One has two CFFs for each GPD H, $\tilde{H}$, E, $\tilde{E}$ → 8 CFFs

Extraction of Compton Form Factors (CFFs)

Quasi-model-independent fitting procedure (M. Guidal, Eur. Phys. J. A 37, 319 (2008)):

→ One does not extract the GPDs, but associated quantities called Compton Form Factors

$$\mathcal{T}^{DVCS} \propto \int_{-1}^{1} dx \frac{GPD(x,\xi,t)}{x \pm \xi \mp i\epsilon} = \mathcal{P}\int_{-1}^{1} dx \frac{GPD(x,\xi,t)}{x \pm \xi} \pm i\pi GPD(x = \mp\xi, \xi, t)$$

Real part **Imaginary part**

→ One has two CFFs for each GPD H, $\tilde{H}$, E, $\tilde{E}$ → 8 CFFs

→ 2 independent observables, 8 unknowns (the CFFs):

→ Non-linear problem, strong correlations

→ Bounding the domain of variation of the CFFs (5xVGG)

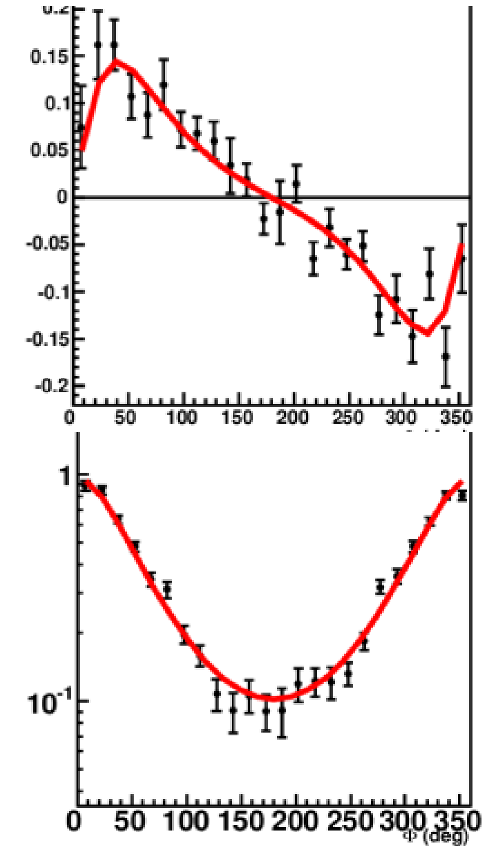

→ At fixed $(Q^2, x_B, -t)$, extraction of the CFFs from the unpolarized and polarized cross sections (x189 bins) with MINUIT + MINOS.

Extraction of Compton Form Factors (CFFs)

Quasi-model-independent fitting procedure (M. Guidal, Eur. Phys. J. A 37, 319 (2008)):

$\rightarrow$ One does not extract the GPDs, but associated quantities called Compton Form Factors

$$\mathcal{T}^{DVCS} \propto \int_{-1}^{1} dx \frac{GPD(x,\xi,t)}{x \pm \xi \mp i\epsilon} = \mathcal{P}\int_{-1}^{1} dx \frac{GPD(x,\xi,t)}{x \pm \xi} \pm i\pi GPD(x = \mp\xi, \xi, t)$$

Real part **Imaginary part**

$\rightarrow$ One has two CFFs for each GPD H, $\tilde{H}$, E, $\tilde{E}$ $\rightarrow$ 8 CFFs

$\rightarrow$ 2 independent observables, 8 unknowns (the CFFs):

$\rightarrow$ Non-linear problem, strong correlations

$\rightarrow$ Bounding the domain of variation of the CFFs (5xVGG)

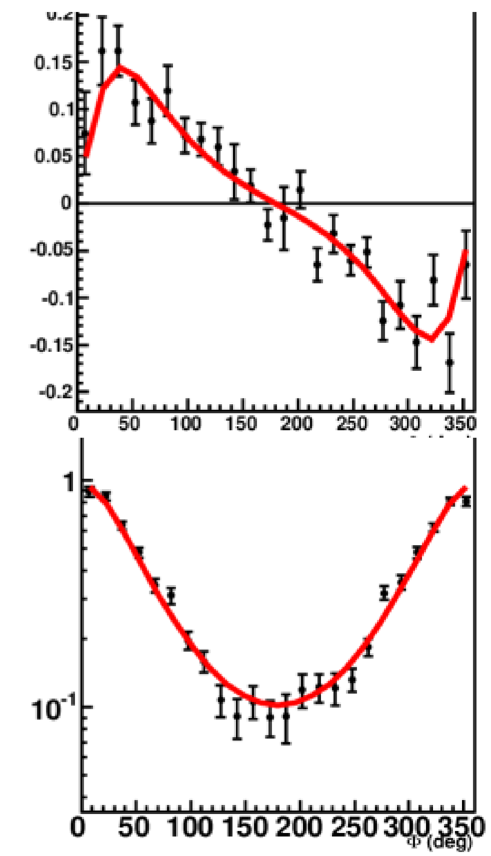

$\rightarrow$ At fixed $(Q^2, x_B, -t)$, extraction of the CFFs from the unpolarized and polarized cross sections (x189 bins) with MINUIT + MINOS.

$\rightarrow$ Extraction of the real part and the imaginary part of the GPD H $\rightarrow$ $\boxed{\mathcal{H}_{Im} \mathcal{H}_{Re}}$

Extraction of Compton Form Factors (CFFs)

Imaginary part of the CFF *H* for four values of *x*:

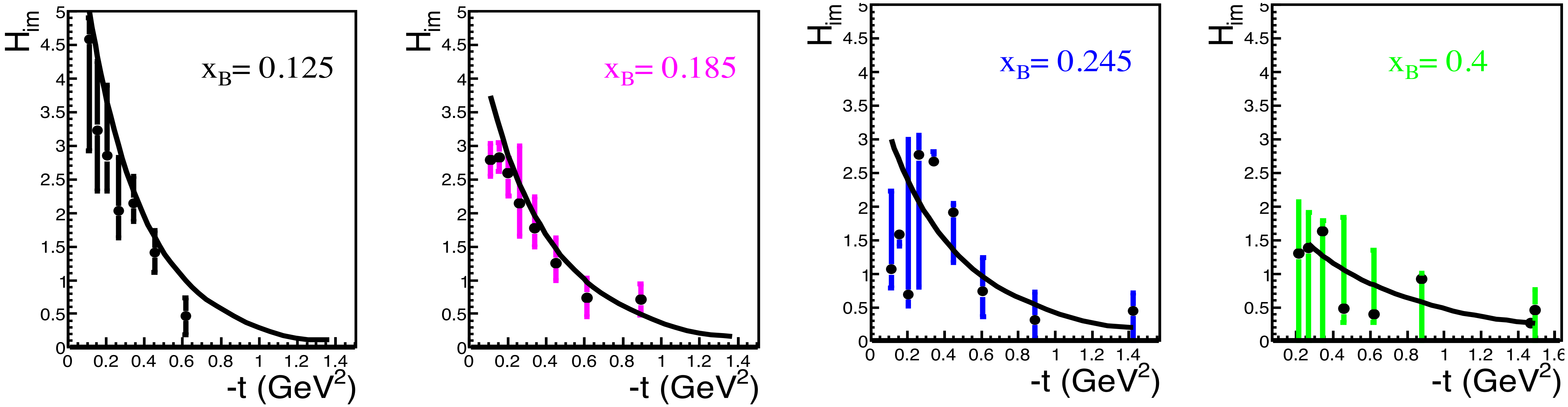

● Results of model-independent fit — VGG model prediction

From CFFs to spatial densities

- $\mathcal{H}_{Im}$ is a combination of GPDs at the line: $x = \pm\xi$

  Neglecting the antiquark contribution $\rightarrow$ $H_{Im}(\xi, t) = H(\xi, \xi, t)$

<u>Density distribution:</u> $\rho(x=\xi, b) = \int_0^\infty \frac{dt}{4\pi} J_0(b\sqrt(t))H(x=\xi, 0, t)$ M. Burkardt Phys.Rev. D 62, 071503 (2000)

BUT: $H(\xi, 0, t) \neq H(\xi, \xi, t)$

Model dependent correction factors (VGG):

$$\rightarrow \frac{H(\xi, 0, t)}{H(\xi, \xi, t)}$$

Effect is $< 20\%$

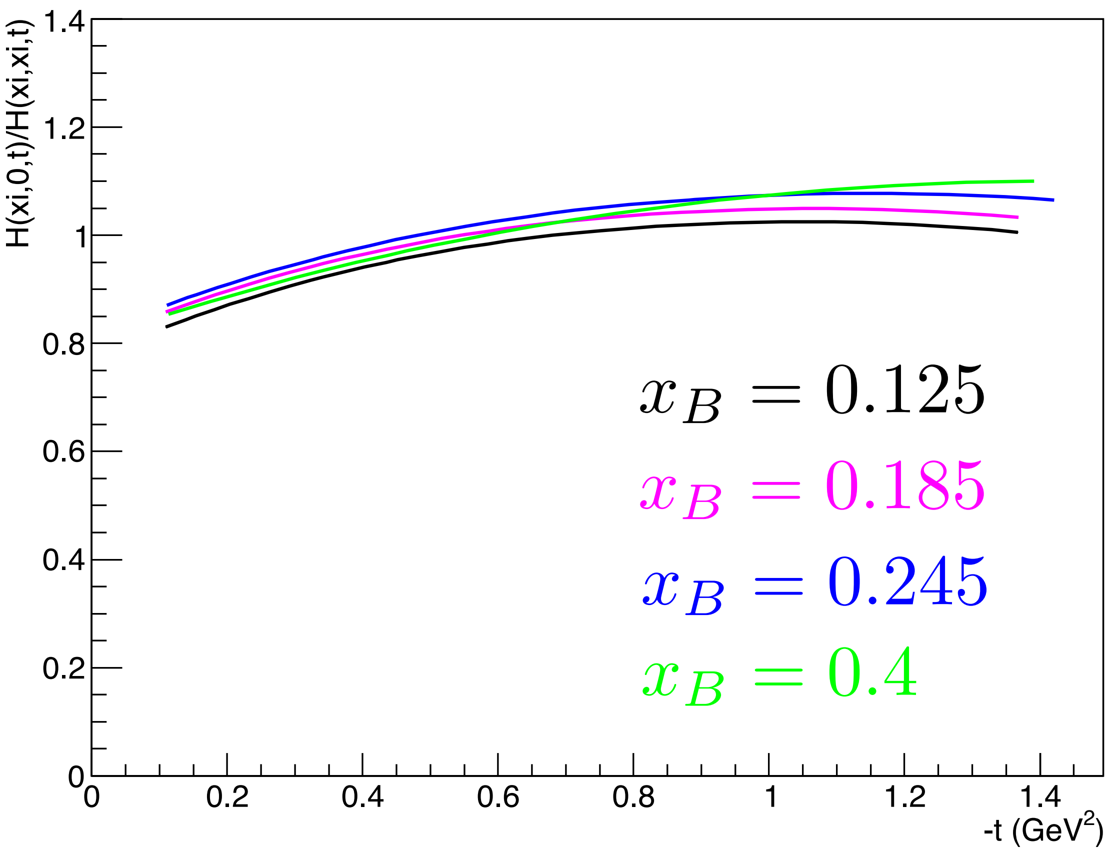

From CFFs to spatial densities

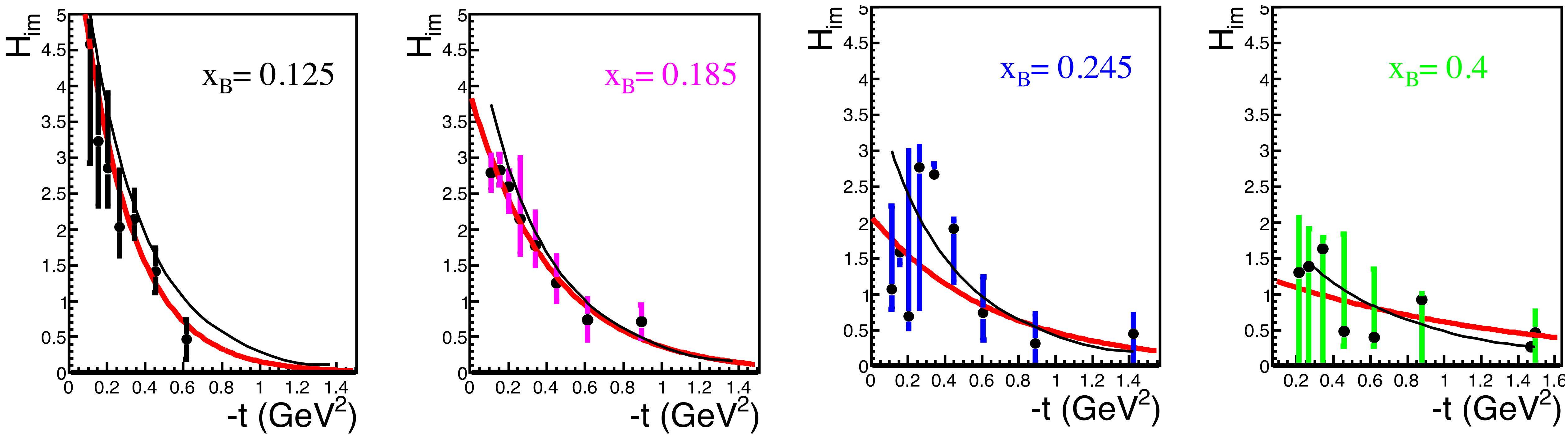

Fit of the t-dependence of H_{Im} with: e^{a+bt} (uncorrected)

From CFFs to spatial densities

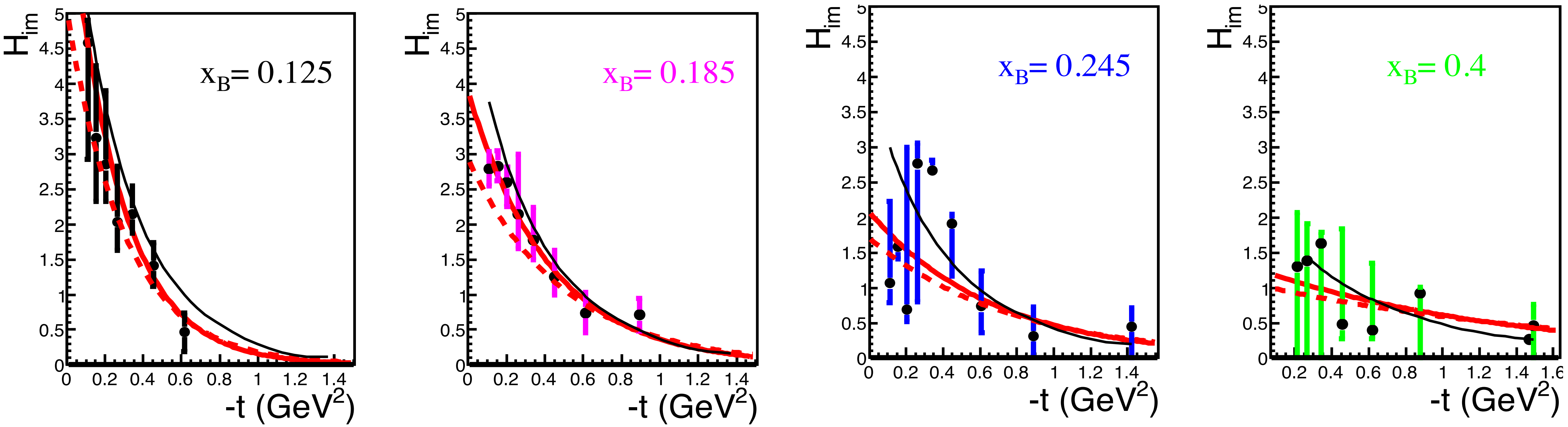

Fit of the t-dependence of H_{Im} with: e^{a+bt} (uncorrected)

Fit of the t-dependence of H_{Im} with: e^{a+bt} (corrected)

From CFFs to spatial densities

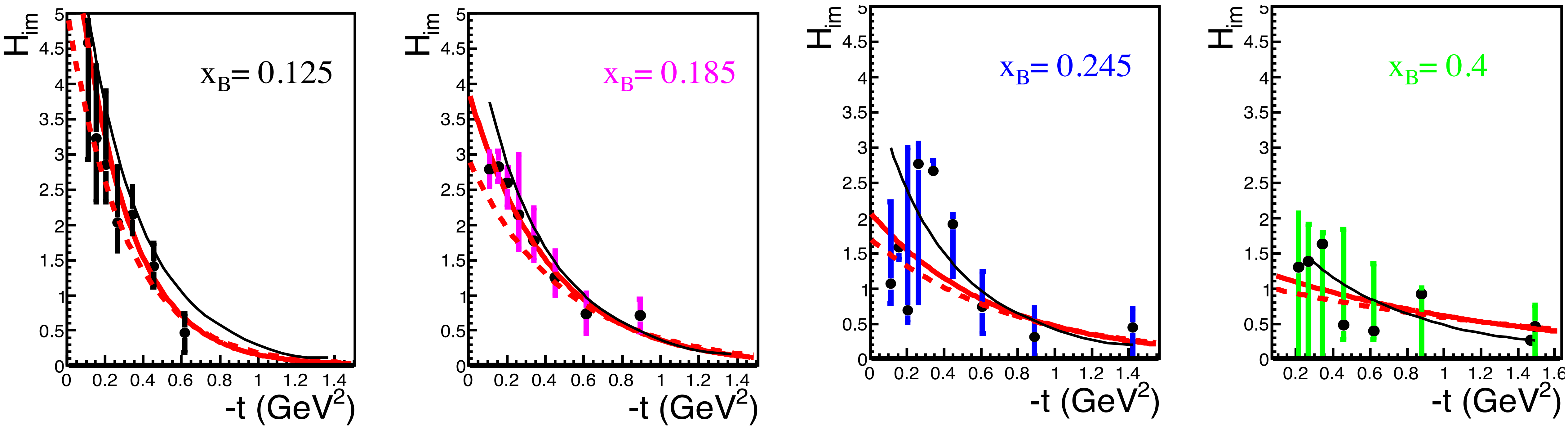

$$\rho(x = x_B, b) = \int_0^\infty \frac{dt}{4\pi} J_0(b\sqrt(t))H(x = x_B, 0, t)$$

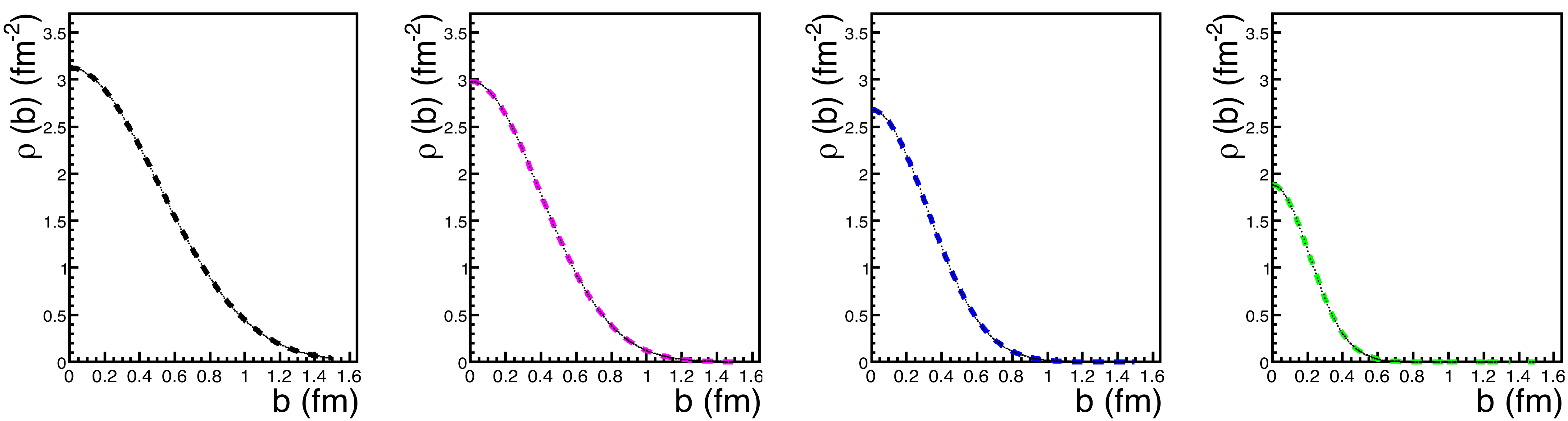

From CFFs to spatial densities

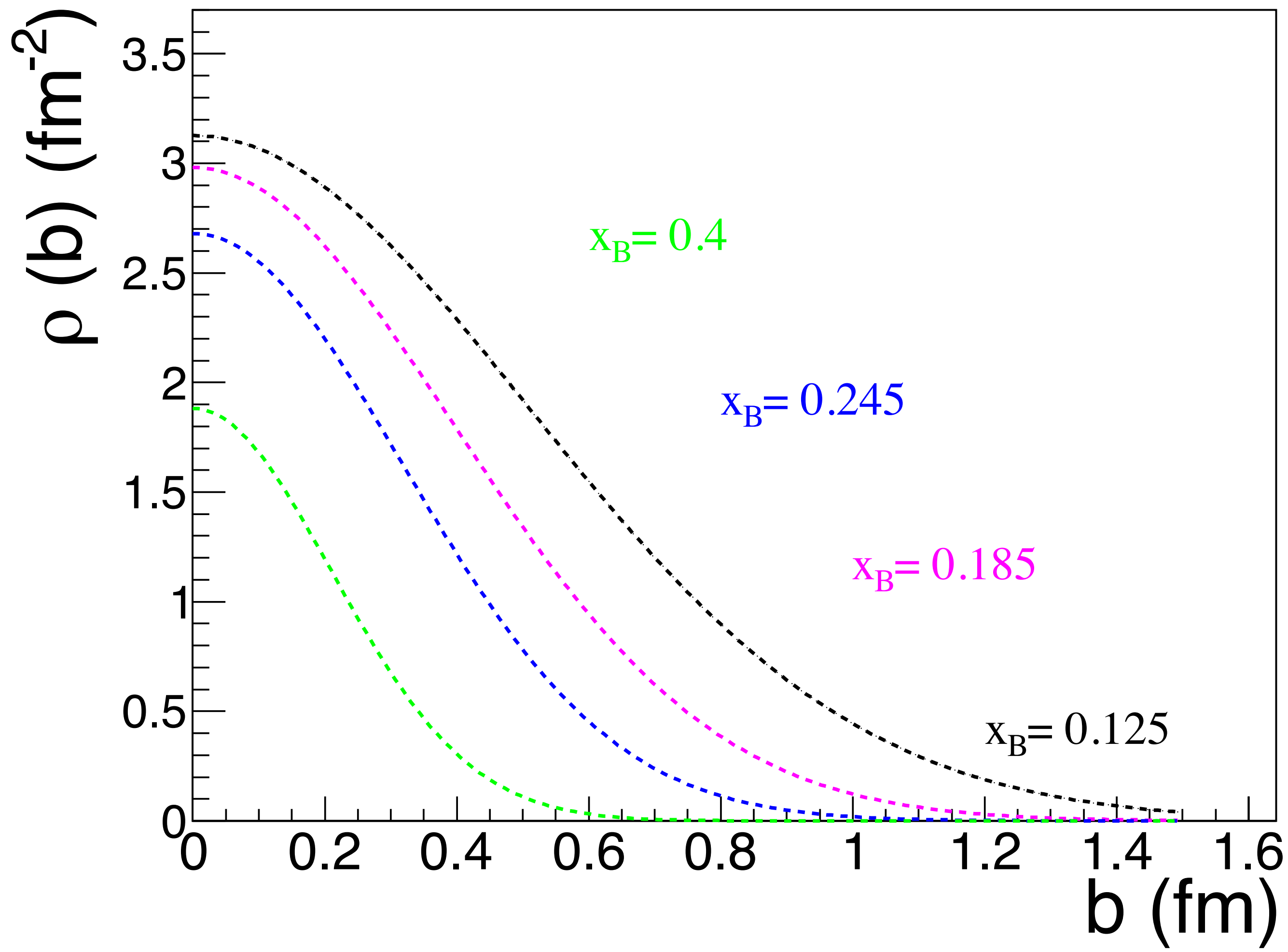

$\mathcal{H}_{Im}$: Correlation between transverse position and longitudinal momentum

➡ The sea quarks (low x) spread to the periphery of the nucleon

➡ The valence quarks (large x) remain in the center

Summary and outlook

- GPDs are a unique tool to explore the internal landscape of the nucleon:
  $\rightarrow$ 3D quark/gluon imaging of the nucleon
- Extraction of DVCS unpolarized and polarized cross sections in the largest kinematic domain ever explored in the valence region
- Extraction of the spatial densities as a function of x
- Analyses in the final stage to extract A_{UL} and $A_{LL}\,(H, \tilde{H})$ from CLAS data at 6 GeV with longitudinally-polarized target
- Dedicated GPD program at Jlab 12GeV:
  Target spin asymmetry: A_{UT} , A_{LT}
  Beam/Target spin asymmetries: A_{UL} , A_{LU}
  DVMP: pseudoscalar/vector mesons

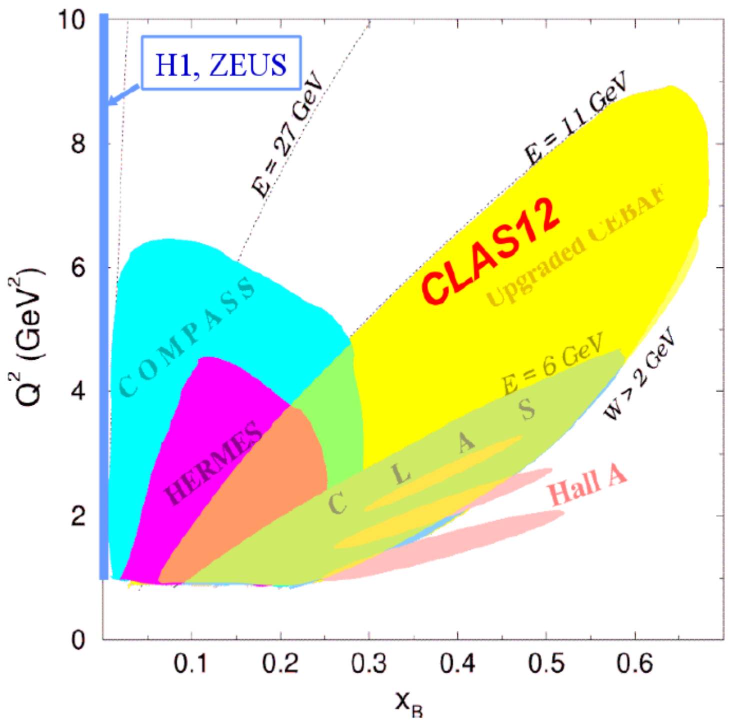

$$\mathcal{T}^{DVCS} \propto \int_{-1}^{1} dx \frac{f(x,\xi,t)}{x \pm \xi \mp i\epsilon} = \mathcal{P}\int_{-1}^{1} dx \frac{f(x,\xi,t)}{x \pm \xi} \pm i\pi f(x = \mp\xi, \xi, t)$$

Real part	Imaginary part
$\mathcal{H}_{Re}(\xi,t) = \mathcal{P}\int_0^1 dx[H(x,\xi,t) - H(-x,\xi,t)]\,C^+(x,\xi)$	$\mathcal{H}_{Im}(\xi,t) = H(\xi,\xi,t) - H(-\xi,\xi,t)$
$\mathcal{E}_{Re}(\xi,t) = \mathcal{P}\int_0^1 dx[E(x,\xi,t) - E(-x,\xi,t)]\,C^+(x,\xi)$	$\mathcal{E}_{Im}(\xi,t) = E(\xi,\xi,t) - E(-\xi,\xi,t)$
$\tilde{\mathcal{H}}_{Re}(\xi,t) = \mathcal{P}\int_0^1 dx[\tilde{H}(x,\xi,t) + \tilde{H}(-x,\xi,t)]\,C^-(x,\xi)$	$\tilde{\mathcal{H}}_{Im}(\xi,t) = \tilde{H}(\xi,\xi,t) + \tilde{H}(-\xi,\xi,t)$
$\tilde{\mathcal{E}}_{Re}(\xi,t) = \mathcal{P}\int_0^1 dx[\tilde{E}(x,\xi,t) + \tilde{E}(-x,\xi,t)]\,C^-(x,\xi)$	$\tilde{\mathcal{E}}_{Im}(\xi,t) = \tilde{E}(\xi,\xi,t) + \tilde{E}(-\xi,\xi,t)$

With: $C^{\pm}(x,\xi) = \frac{1}{x-\xi} \pm \frac{1}{x+\xi}$

	Sensitivity	Experiment
$\sigma_{unp} = \sigma^{\rightarrow} + \sigma^{\leftarrow}$	$\propto \mathcal{H}_{Re}$	H1 ((2001), (2005), (2008)) ZEUS ((2003) , (2009)) Hall-A (2006) Hall-B (E1-DVCS experiment: data under analysis)
$\sigma_{pol} = \sigma^{\rightarrow} - \sigma^{\leftarrow}$	$\propto \mathcal{H}_{Im}$	Hall-A (2006) Hall-B (E1-DVCS experiment: data under analysis)
$\mathcal{A}_C$	$\propto \mathcal{H}_{Re}$	HERMES ((2007) , (2008) , (2009))
$\mathcal{A}_{LU}$	$\propto \mathcal{H}_{Im}$	HERMES ((2001) , (2009)) Hall-B ((2001) , (2008))
$\mathcal{A}_{UL}$	$\propto \mathcal{H}_{Im}, \tilde{\mathcal{H}}_{Im}$	Hall-B (2006) HERMES (2010) Hall-B (Eg1-DVCS experiment: data under analysis)
$\mathcal{A}_{LL}$	$\propto \mathcal{H}_{Re}, \tilde{\mathcal{H}}_{Re}$	HERMES (2010) Hall-B (Eg1-DVCS experiment: data under analysis)
$\mathcal{A}_{UT}$	$\propto \mathcal{E}_{Im}$	HERMES (2008) Hall-B proposal
$\mathcal{A}_{LT}$	$\propto \mathcal{H}_{Re}, \mathcal{E}_{Re}$	HERMES (2011) Hall-B proposal

- The second moment of (E+H) when t → 0 : total angular momentum

$$\int_{-1}^{1} dx\, x\,[H^q(x,\xi,0)+E^q(x,\xi,0)] = 2\boxed{J_{quarks}}$$ (Ji sum rule)

Nucleon spin decomposotion: $\frac{1}{2} = J_{quarks} + J_{gluons} = \boxed{S_{quarks} + L_{quarks}} + S_{gluons} + L_{gluons}$

$EMC: \approx 30\,\%$ $COMPASS, STAR, PHENIX: \approx 0\,\%$

- At ξ = 0, a GPD is a x-decomposition of the form factor:

→ u-quark distribution in a unpolarized proton

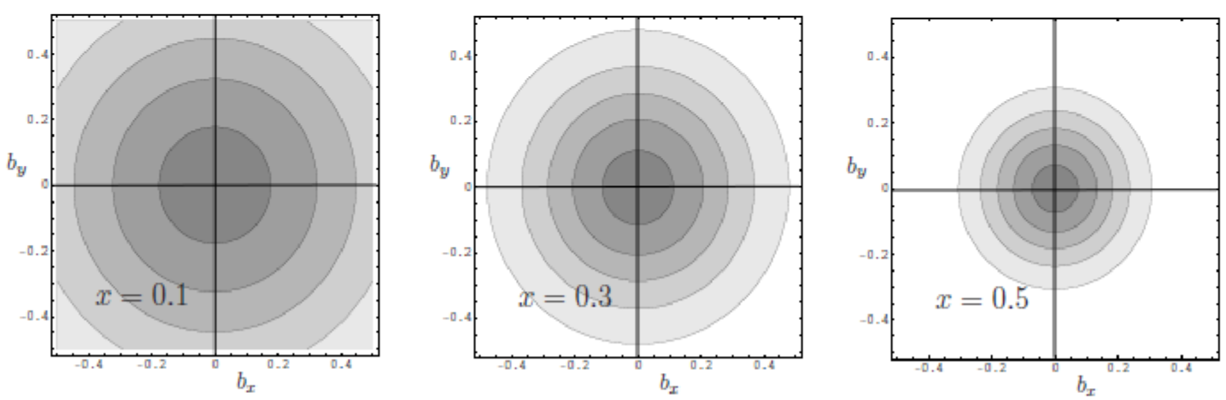

$$q(x,0,b_\perp) = \int \frac{d^2\Delta_\perp}{(2\pi)^2} e^{ib_\perp\Delta_\perp} H^q(x,0,-\Delta_\perp^2)$$

→ u-quark distribution in a polarized proton

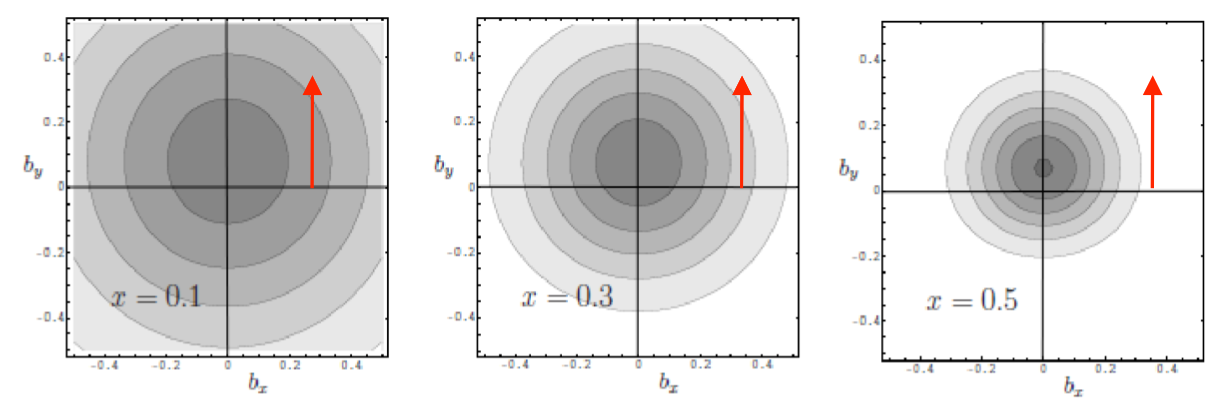

$$q_{+X}(x,0,b_\perp) = q(x,0,b_\perp) - \frac{1}{2M}\frac{\partial}{\partial b_y}\int \frac{d^2\Delta_\perp}{(2\pi)^2} e^{ib_\perp\Delta_\perp} E^q(x,0,-\Delta_\perp^2)$$

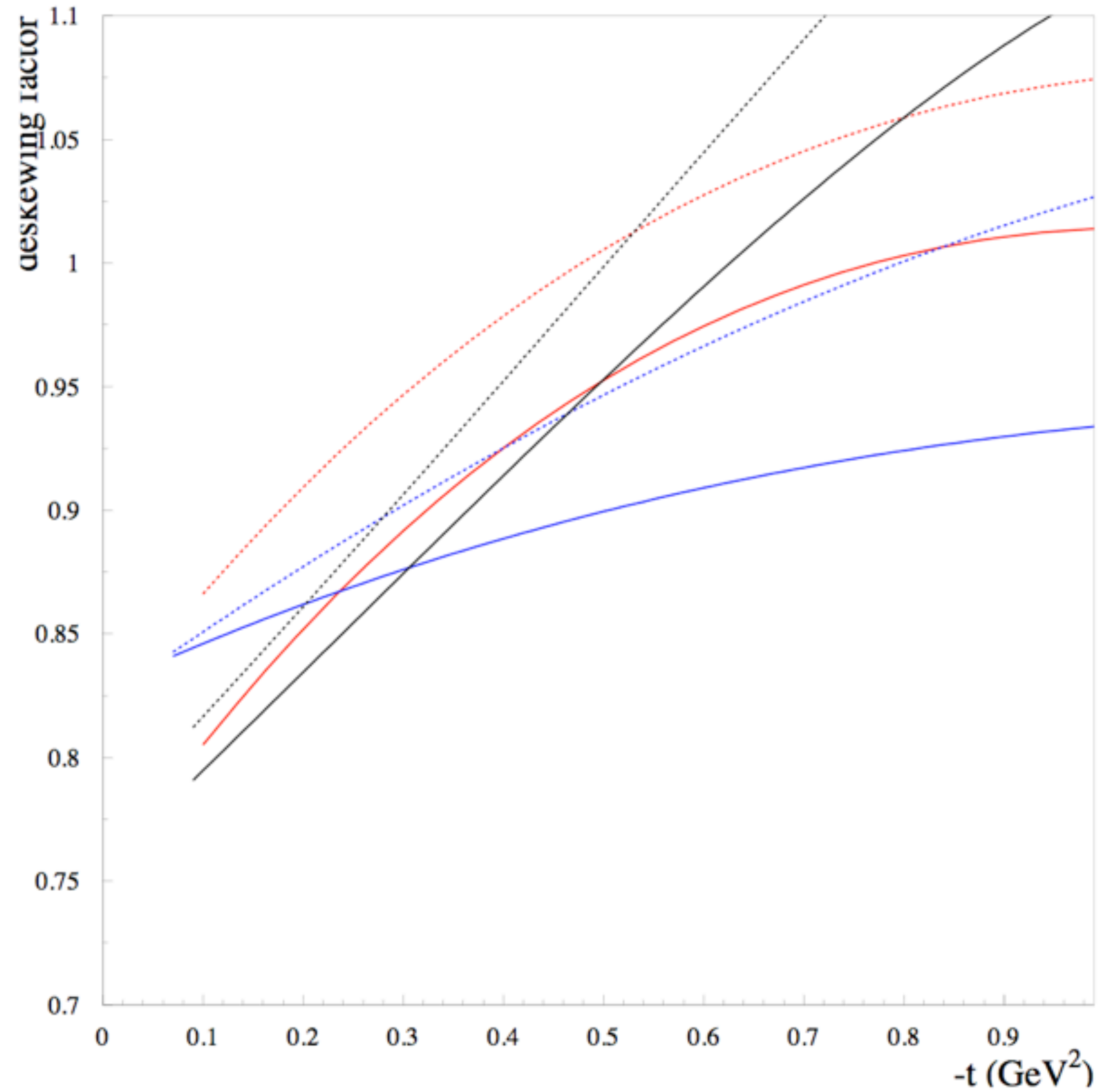

Figure 54. "Deskewing" factor $H(\xi, 0, t)/H(\xi, \xi, t)$ as a function of $-t$ for the VGG model (red curves), the GK model (blue curves) and the dual model (black curves). The solid curves correspond to x_B=0.1 (HERMES kinematics) and the dashed ones to x_B=0.25 (CLAS kinematics).